Chemical Research in Toxicology

ARTICLE

pubs.acs.org/crt

Revisiting the Peroxidase Oxidation of 2,4,6-Trihalophenols: ESR Detection of Radical Intermediates

Bradley E. Sturgeon,*[,†] Benjamin J. Battenburg,[†] Blake J. Lyon,[†] and Stefan Franzen[‡]

[†]Department of Chemistry, Monmouth College, Monmouth, Illinois 61462, United States

[‡]Department of Chemistry, North Carolina State University, Raleigh, North Carolina 27695, United States

Supporting Information

ABSTRACT: The peroxidase oxidation of 2,4,6-trichlorophenol (TCP) has been clearly shown to result in 2,6-dichloro-1,4-benzoquinone (DCQ). DCQ is a 2-electron oxidation product of TCP that has undergone para dechlorination. Many peroxidases show similar oxidation of the substrate, TCP, to yield the quinone, DCQ. Depending on the substrate, peroxidases are thought to carry out both 1- and 2-electron oxidations; the mechanism can be confirmed by the detection of both enzyme and substrate intermediates. This article presents ESR evidence for the transient 2,4,6-trichlorophenoxyl radical intermediate (TCP•), which exists free in solution, i.e., is not enzyme associated. These data are best explained as a 1-electron peroxidase oxidation of TCP to form TCP•, followed by enzyme-independent radical reactions leading to the 2-electron oxidized product. Also presented are data for the peroxidase oxidation of 2,4,6-trifluorophenol and 2,6-dichloro-4-fluorophenol.

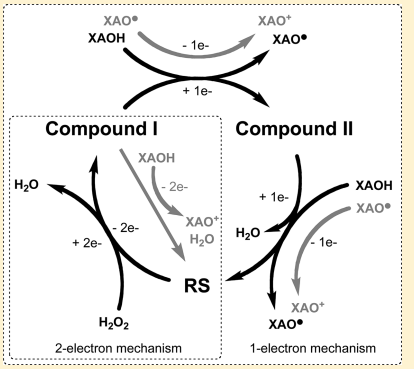

INTRODUCTION

A peroxidase in the presence of H_2O_2 will carry out the oxidization of phenolic compounds such as 2,4,6-trichlorophenol (TCP). In the case of ligin peroxidase,[1] horseradish peroxidase (HRP),[2,3] chloroperoxidase,[4,5] dehaloperoxidase-hemoglobin,[6] and myoglobin,[7] the main product is reported to be 2,6-dichloro-1,4-benzoquinone (DCQ). DCQ is the 2-electron oxidized form of TCP that has undergone para dechlorination (Scheme 1).

The typical peroxidase mechanism is outlined in Figure 1 and is initiated by the 2-electron oxidation of the enzyme resting state (RS) by an oxidizing substrate (eg., H_2O_2) to form compound I. Depending on the origin of the peroxidase, the structural form of compound I consists of Fe(IV)═O and either a heme radical cation or an amino acid radical.[8] Compound I then undergoes a 1-electron reduction by a reducing substrate (eg., a halophenol, XAOH) to form compound II and the corresponding radical, XAO•. Compound II then undergoes a second 1-electron reduction by a second molecule of the reducing substrate to regenerate RS and an additional radical.

This peroxidase mechanism is commonly referred to as an irreversible ping-pong mechanism.[8] The name makes reference to a very short-lived enzyme−substrate complex; the product departs as fast as the substrate contacts the enzyme, like a ping-pong ball when it strikes a paddle. To account for the formation of the 2-electron oxidized product, DCQ, three different pathways/reactions are considered. First, the radical, XAO•, can act as a reducing substrate for compound I and/or compound II forming a transient cyclohexadienone cation (XAO^+). XAO^+ would rapidly react with water (or OH^-), dehalogenate, and result in the quinone product (O═A═O)[1−4,7](Figure 1, 1-electron mechanism). Second, the reducing substrate (eg., XAOH) can act as a 2-electron reducing substrate for compound I, hence forgoing the formation of compound II, and resulting in XAO^+, then the quinone (Figure 1, 2-electron mechanism). Third, the radical generated via 1-electron oxidation of TCP can undergo an apparent radical−radical dismutation reaction resulting in the original reducing substrate and the quinone (reaction 1).

$$2XAO\bullet + H_2O \rightarrow XAOH + O{=}A{=}O + H^+ + Cl^- \quad (1)$$

For a given enzyme/substrate system, it is important to know which mechanism is in operation. The difference between the 1-electron and 2-electron mechanism involves two key points: (1) compound II is formed during the 1-electron mechanism and not during the 2-electron mechanism, and (2) a radical (eg., XAO•) is formed during the 1-electron mechanism and not during the 2-electron mechanism. The significance of which mechanism is in operation can be briefly summarized by the following comments: (1) the formation of radical intermediates provides opportunities for other reactions/products to occur, and (2) the more involved enzyme kinetics of the 1-electron mechanism, the more intermediates that can be targeted to modulate enzyme function.

The 1-electron mechanism has been most frequently used to explain the formation of DCQ.[1−4,7] Compound II oxidation of the reducing substrate is usually the rate limiting step in the enzymatic cycle and hence can be detected under steady-state conditions. In cases where the form of compound II involves the

Received: May 21, 2011
Published: September 27, 2011

Scheme 1. Peroxidase oxidation of 2,4,6-trichlorophenol to form the quinone product

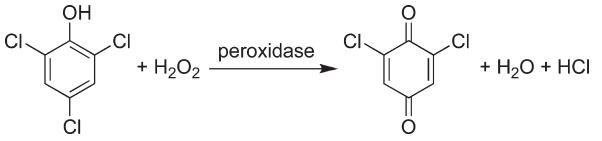

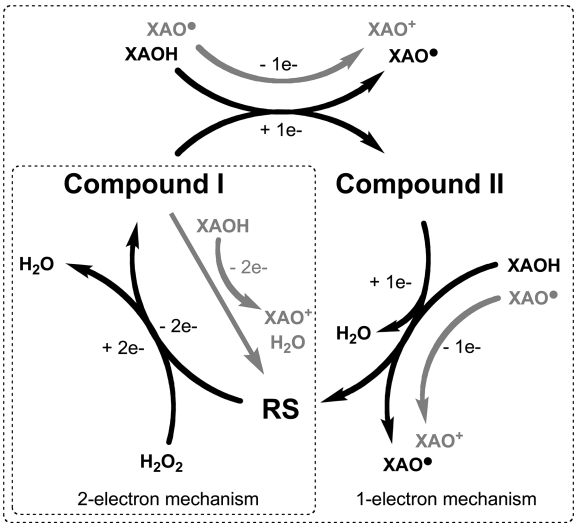

Figure 1. Outline of peroxidase mechanism with H_2O_2 as the oxidizing substrate and a halophenol (XAOH) as the reducing substrate. Enzyme intermediates are labeled as resting state (RS), compound I, and compound II. The dotted borders indicate the reactions specifically involved in the 1-electron and 2-electron mechanisms. Reactions presented in gray lead to the formation of a quinone (a two-electron oxidized product).

heme radical cation, UV−vis detection is fairly straightforward, although when the form of compound II involves a protein radical, UV−vis detection is more challenging.[9] This 1-electron mechanism is also supported by the observation of compound II under single-turnover conditions; if the 2-electron mechanism were involved, compound II would not be detected as is the case for the oxidation of thioanisole by CCPO,[5] iodide by HRP,[10] and sulfite by HRP.[11]

In this article, we present ESR data related to the reaction of HRP/H_2O_2 with TCP and other TCP-analogues and present evidence to support the 1-electron oxidation mechanism mediated by both enzyme and radical chemistry.

EXPERIMENTAL PROCEDURES

Materials. HRP (Type-VIa), TCP, TFP, DCFP, and horse heart myoglobin were obtained from Sigma Chemical Company (St. Louis, MO). Dehaloperoxidase was purified as described previously.[12] All other chemicals were of the highest purity available.

UV−Visible Spectroscopy. The oxidation of TCP by HRP/H_2O_2 was followed using an HP8453 photodiode array UV−visible spectrometer. A cuvette containing TCP and H_2O_2 was scanned (230−400 nm) prior to the addition of enzyme (t = 0 s). The reaction was initiated by the addition of a negligible volume of HRP, mixed, and scanned at 30 s; additional scans were taken every 30 s. Since the absorption of TCP was well separated from DCQ, data were analyzed using the method presented by Harris[13] using the data in Table 1.

Table 1. Molar Absorptivity Values Used to Generate Concentration Data in Figure 3

	TCP		DCQ	
pH	ε_{274}[a]	ε_{312}[a]	ε_{274}[a]	ε_{312}[a]
6.2	1.18	3.39	12.64	0.43
7.4	0.96	4.17	12.17	0.41
9.0	1.03	4.58	8.37	1.89

[a] In units of mM^{-1} cm^{-1}.

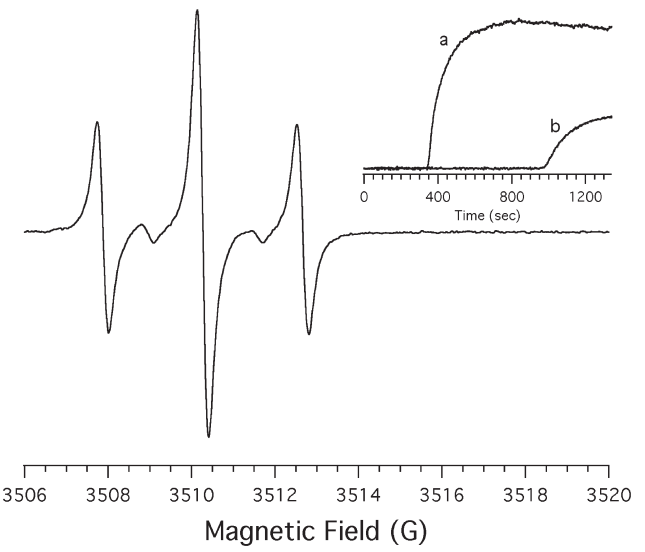

Figure 2. ESR spectrum observed 13 min after a solution of HRP (4.47 μM), H_2O_2 (0.5 mM), and TCP (0.5 mM) at pH 7.4 was mixed and transferred to the mounted Aqua-X ESR sample holder. The inset monitors the ESR intensity at 3510 G vs time for (a) 4.47 μM HRP and (b) 0.447 μM HRP. ESR parameters: 9.85 GHz microwave frequency, 1 mW microwave power, 100 kHz modulation frequency, 0.2 G_{pp} modulation amplitude, and 82 s scan time with a 164 ms time constant.

ESR Spectroscopy. Detection of all radicals was done using a Bruker EMX spectrometer (Billerica, MA) equipped with a High Sensitivity cavity. X-band (~9.8 GHz) ESR conditions are listed in the figure captions. When detecting radicals from a standard mixing experiment (Figure 2), the sample was introduced into the cavity using the Bruker Aqua-X sample holder. When conducting IE-ESR experiments, enzymes were loaded into a WG-812-Q flatcell from Wilmad Glass (Vineland, NJ) as described.[14] ESR simulations were performed using the WINSIM program;[15] all presented simulations use best-fit parameters as determined by the WINSIM program.

RESULTS

Shown in Figure 2 is the ESR spectrum detected when a solution of TCP/H_2O_2 (pH 7.4) was mixed with HRP and quickly (~20 s) transferred into the ESR spectrometer. The resulting spectrum (a^H = 2.4 G) is equivalent to the ESR spectrum previously detected by Wiese et al. and is unlikely to be TCP•.[2] The time course for the observed radical is shown in the inset of Figure 2. The radical signal was not detected immediately and was dependent on HRP concentration. At 4.47 μM HRP (Figure 2, inset a), the radical signal appeared at ~350 s after mixing, whereas at 0.447 μM HRP (Figure 2, inset b), the radical signal appeared at ~970 s after mixing. Previous work

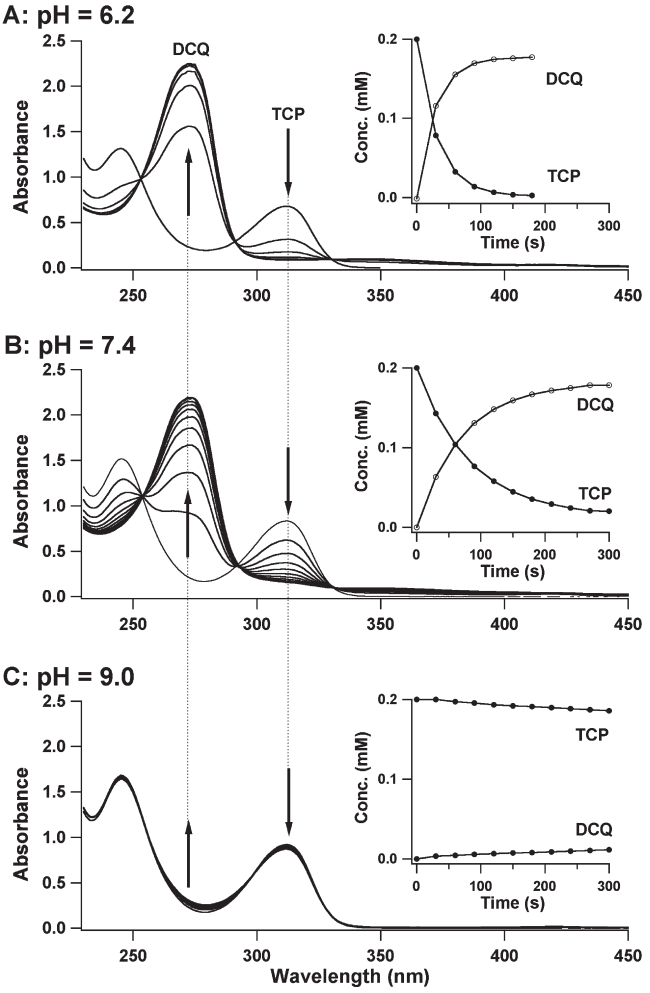

Figure 3. UV−visible monitoring of TCP oxidation by HRP and H_2O_2. Solutions contained HRP (0.2 μM), H_2O_2 (0.2 mM), and TCP (0.2 mM) at A, pH 6.2, B, pH 7.4, and C, pH 9.0. Inset data are the calculated concentration of TCP and DCQ as described in the Experimental Procedures.

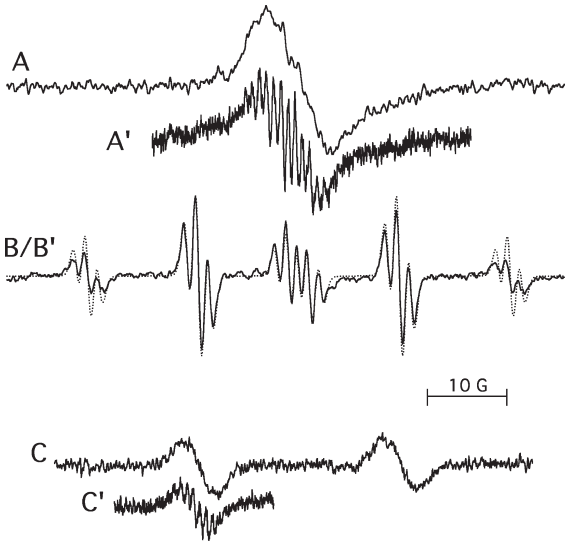

Figure 4. IE-ESR spectra collected using HRP_i/H_2O_2 and halophenols at pH 7.4. (A) ESR spectrum of TCP• (g = 2.008) collected using HRP_i (3 mg/mL), H_2O_2 (1 mM), TCP (0.5 mM), and a 2.0 mL/min flow rate. ESR parameters: 9.798 GHz microwave frequency, 20 mW microwave power, 1 G_{pp} modulation amplitude, and an average of 10−42 s scans with a time constant of 82 ms; (A′) high-resolution TCP• collected using the same conditions as A but with 0.5 G_{pp} moduation amplitude and an average of 20−167 s scans with a time constant of 167 ms; (B) TFP• (g = 2.006) collected using HRP_i (3.0 mg/mL), H_2O_2 (1 mM), TFP (1.0 mM), and a 2.0 mL/min flow rate. ESR parameters: 9.802 GHz microwave frequency, 20 mW microwave power, 1 G_{pp} modulation amplitude, and an average of 10−84 s scans with a time constant of 164 ms; (B′) overlay of simulation (dotted) ESR spectrum, see text for simulation parameters; (C), DCFP• (g = 2.005) collected using HRP_i (0.7 mg/mL), H_2O_2 (1 mM), DCFP (0.5 mM), and a 2.0 mL/min flow rate. ESR parameters: 9.775 GHz microwave frequency, 20 mW microwave power, 2 G_{pp} modulation amplitude, and an average of 10−42 s scans with a time constant of 82 ms; and (C′) high-resolution DCFP• collected using the same conditions as those in C, except for 0.5 G_{pp} modulation amplitude and an average of 110−42 s scans with a time constant of 82 ms.

by Wiese et al.[2] used 23 μM HRP, which apparently resulted in an almost immediate detection of this radical signal. The effect of TCP or H_2O_2 concentration on the time course of the radical was not investigated. Similar attempts at ESR data collected with HRP (0.447 μM), TCP, and H_2O_2 at pH 6.2 and 9.0 observed no radical within a 40 min period. The time course of this reaction was followed by UV−visible spectroscopy at pH 6.2, 7.4, and 9.0 (Figure 3) indicating that oxidation of TCP was rapid at pH 6.2 and pH 7.4, although quite slow at pH 9.0.

Although the published TCP• ESR hyperfine couplings[2] are consistent with a diortho substituted phenoxyl radical, in the case of TCP• two questions arise: (1) the time course for the radical formation/persistence is unexpected for a phenoxyl radical, and (2) the spectrum is missing chlorine hyperfine couplings. Chlorine hyperfine couplings often go undetected since the gyromagnetic ratios for ^{35}Cl and ^{37}Cl are quite small (and different for each isotope), which typically result in inhomogeneous line broadening. As for the time course, a phenoxyl radical like TCP• is expected to form during the early events of the enzymatic cycle and is expected to be considerably less stable (more reactive) than the observed radical signal. The lack of chlorine hyperfine combined with the peculiar radical persistence lead us to investigate further the early events in the enzymatic cycle.

In order to observe highly reactive radicals formed during the early events of the enzymatic cycle, the ESR techniques of fast-flow ESR or immobilized enzyme ESR (IE-ESR) are required.[14] Shown in Figure 4A is the IE-ESR spectrum observed when a TCP/H_2O_2 solution (pH 7.4) was flowed over immobilized HRP (HRP_i). Under these experimental conditions, radicals with lifetimes of milliseconds have been detected.[14,16,17] The very broad, featureless spectrum (Figure 4A) provides no clear information with respect to the identification of TCP•, although when ESR conditions were set to be sensitive to spectral features and not signal-to-noise (i.e., modulation amplitude changed from 1.0 G_{pp} to 0.5 G_{pp} with signal averaging), the ESR spectrum shown in Figure 4A′ was observed. This spectrum showed clear hyperfine interactions that can be simulated (Figure S1, Supporting Information) using two *ortho*-chlorine hyperfine coupling constants (hfcc) (a_o^{Cl} = 0.90 G), a *para*-chlorine hfcc (a_p^{Cl} = 1.82 G), and two *meta*-proton hfcc (a_m^{H} = 1.62 G); this spectrum and simulation are consistent with the TCP• formed in organic solvents by photolysis.[18]

In order to overcome the complexity associated with chlorine nuclei, the same IE-ESR experiments were performed with the

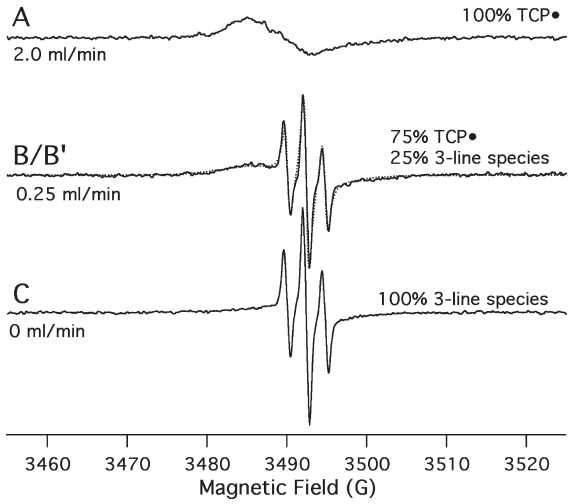

Figure 5. IE-ESR spectra collected at varying substrate flow rates for HRP_i/H_2O_2/TCP at pH 7.4. (A) ESR spectrum of TCP• at 2.0 mL/min, same data as that presented in Figure 4A; (B) same as A, except for 0.25 mL/min; (B′) simulation of B with relative contribution of TCP• and the three-line spectrum indicated; (C) same as A, except for the flow is stopped, and only 5 scans are averaged.

fluoro-analogue of TCP, 2,4,6-trifluorophenol (TFP). Shown in Figure 4B is the IE-ESR spectrum observed when a TFP/H_2O_2 solution (pH 7.4) was flowed over HRP_i. Similar spectra were observed when enzymatic oxidation was carried out by dehaloperoxidase or myoglobin (Figure S2, Supporting Information). Unlike TCP, this ESR spectrum was rich in hyperfine couplings. On the basis of previous ESR data on the tyrosyl radical[19] and the phenoxyl radical,[20] the observed ESR spectra can be simulated (Figure 4B′) using two large *ortho*-fluorine hfcc (a_o^F = 13.5 G), an even larger *para*-fluorine hfcc (a_p^F = 25.0 G), and two *meta*-proton hfcc (a_m^H = 1.5 G). Additionally, IE-ESR data were collected for the peroxidase oxidation of 2,6-dichloro-4-fluorophenol (DCFP). When a DCFP/H_2O_2 solution (pH 7.4) was flowed over HRP_i, a doublet ESR spectrum was observed with a single hfcc (a_p^F = 25.2 G) assigned to the *para*-fluorine nuclei (Figure 4C). When ESR conditions were set to be sensitive to spectral features and not signal-to-noise (ie., modulation amplitude changed from 2 G_{pp} to 0.5 G_{pp} with signal averaging), as was done with TCP•, the ESR spectrum revealed clear hyperfine interactions (a_o^{Cl} = 0.84 G and a_m^H = 1.44 G) consistent with the values observed in TCP• (Figure 4A′). The simulation (low field only) of the DCFP• radical spectrum is presented in Figure S1 of the Supporting Information. IE-ESR experiments were performed under acidic conditions (pH 5) for TCP, TFP, and DCFP; the ESR spectra were nearly identical to the pH 7.4 data. No high resolution ESR data were collected at pH 5. No IE-ESR data were collected under basic (pH∼9) conditions since UV−vis data (Figure 3) showed that the enzymatic activity was low.

A unique aspect of the IE-ESR experiment is that when the substrate (XAOH/H_2O_2) flow rate is high (2 mL/min), early time (msec) events are observed. When flow rates are decreased, additional chemistry is allowed to occur in the active region of the ESR detection system. Shown in Figure 5 are the ESR spectra collected under a set of different flow conditions for HRP_i/H_2O_2/TCP. The most obvious result was that the ESR signal (a^H=2.4 G) seen under slow-flow (0.25 mL/min) (Figure 5B) and stopped-flow conditions (Figure 5C) is nearly identical to

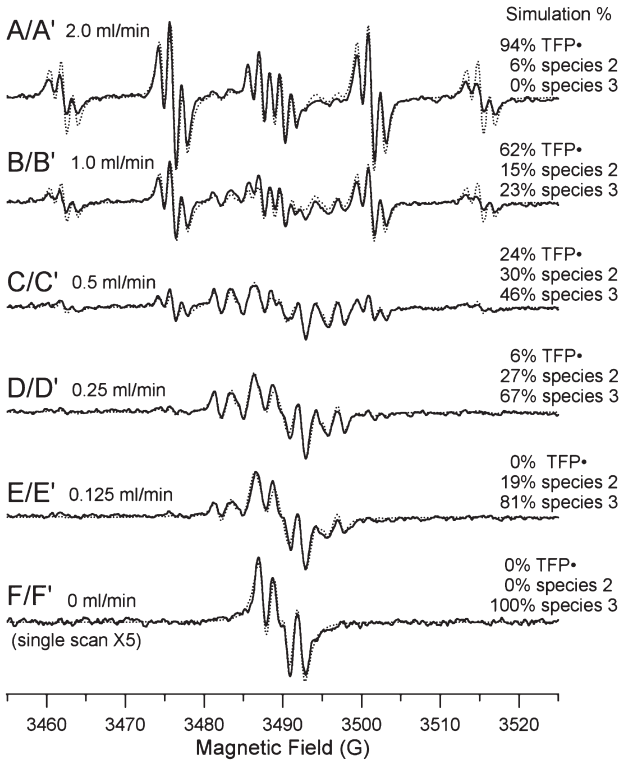

Figure 6. IE-ESR data collected for HRP_i (8 mg/mL)/H_2O_2 (1.0 mM)/TFP (1.0 mM) at varying substrate flow rates and the simulated ESR data. All data were collected using the same ESR data acquisition parameters. The hyperfine coupling constants used in the simulations are presented in the text; the % contribution to the overall spectrum is stated on the Figure. (A) 2.0 mL/min with ESR parameters similar to those in Figure 4B; (A′) simulation of A; (B) 1.0 mL/min; (B′) simulation of B; (C) 0.50 mL/min; (C′) simulation of C; (D) 0.25 mL/min; (D′) simulation of D; (E) 0.125 mL/min; (E′) simulation of E; (F) 0 mL/min; and (F′) simulation of F.

the ESR signal detected under standard mixing conditions (Figure 2). This result suggests that the radical seen under standard mixing conditions is not the primary phenoxyl radical but a secondary radical species. At an intermediate flow rate of 0.25 mL/min (Figure 5B), both the primary phenoxyl radical and the secondary radical are visible. Note the differences in radical *g*-values.

When variable flow rate IE-ESR data were collected for the HRP_i/H_2O_2/TFP system (Figure 6), the resolved fluorine hyperfine allowed for the observation of additional radical species. All of the data in Figure 6 can be simulated using three different radical species; species 1 (TFP•) [$a_m^H(2)$ = 1.42 G, $a_o^F(2)$ = 13.90 G, and $a_p^F(1)$ = 25.08 G], species 2 [$a(1)$ = 1.99 G, $a(1)$ = 2.86 G, and $a(1)$ = 10.7 G], and species 3 [$a(1)$ = 1.86 G and $a(1)$ = 2.92 G].

DISCUSSION

The observation of the chlorine and fluorine hyperfine on the primary radicals generated from the HRP_i/H_2O_2/TCP, HRP_i/H_2O_2/TFP, and HRP_i/H_2O_2/DCFP systems is clear evidence of a 1-electron peroxidase mechanism in HRP; we believe this to be the case with dehaloperoxidase and myoglobin. This conclusion was correctly presented by Wiese et al.[2] but based on incorrectly assigned ESR data. It is important to stress that the detection of

Scheme 2. Enzyme Independent, Radical−Radical Coupling Reaction Leading to the Quinone Product

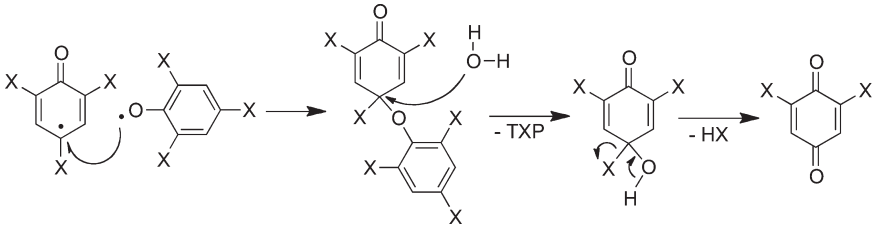

TCP•, TFP•, and DCFP• is support for the 1-electron peroxidase mechanism, although without correlating the radical concentration with H_2O_2 consumed, which is difficult due to high radical reactivity, these results can only say that the 1-electron mechanism is clearly in operation; they do not rule out the 2-electron mechanism. In addition, the detection of such an isotropic (symmetric) ESR spectrum is clear evidence that the radical product is not associated with the reaction center, hence in solution. Our ESR data suggest that a most appropriate mechanism for the formation of DCQ is a combination of 1-electron peroxidase oxidation of the halophenol, followed by the radical−radical coupling chemistry (reaction 1) originally put forth, as one option, by Wiese et al.[2]

The presented ESR data show a large hfcc at the para position, indicating large unpaired spin density; hence, the ether intermediate would be a favorable radical−radical coupling product (Scheme 2). This enzyme/radical mechanism is much more likely than the halophenoxyl radical as a peroxidase substrate since the steady-state concentration of the halophenoxyl radical is quite low compared to the halophenol. This enzyme-independent radical chemistry of the peroxidase-generated radicals commonly dictates product formation as with the case of the tyrosyl radical forming dimers and trimers[21] and ascorbate radical dismutation.[22]

So, what is the origin of the radical shown in Figure 2 and presented by Wiese et al.?[2] We believe that the radical shown in Figure 2 is 2,6-dichloro-1,4-benzosemiquinone for the following reasons: (1) the radical's persistence is consistent with those observed for chlorinated benzosemiquinones;[23] (2) the observed 1:2:1 structure of the ESR spectrum is consistent with the expected hfcc for the two equivalent ring protons; (3) the absence of the chlorine hyperfine is an indication of small couplings that will contribute to only line width;[23,24] and (4) the radical shown in Figure 2 was not observed when the reaction was carried out at pH < 6.2; benzosemiquinones are known to not persist at or below pH values <pK_a of the benzosemiquinone.[25]

As presented in Figures 5 and 6, the IE-ESR method can vary the flow rate to detect secondary radicals. We were hopeful that the detection of secondary radicals for the fluoro-analogue of TCP (TFP•) would assist in the analysis of the TCP• secondary radical, although this was not the case. If the TFP• under went the same radical evolution as TCP•, then the final ESR spectrum seen under 0 mL/min flow conditions (Figure 6F) would have been from the unique 2,6-difluoro-1,4-benzosemiquinone. Apparently, the oxidation of TFP does not only result in para dehalogenation, as is the case with the oxidation of TCP,[1−3] but also in ortho dehalogenation as well. It is important to note that since the 0 mL/min flow ESR spectrum for TCP oxidation does not show any chlorine hyperfine splitting, these data cannot be used to prove that dechlorination does not occur at the ortho

Scheme 3. Proposed Radical Evolution Based on ESR Data in Figure 6

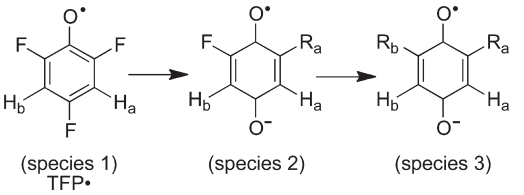

positions. Hammel and Tardone[1] have reported that only one inorganic chloride per TCP is detected during the peroxidase oxidation of TCP; hence, this result alone has led to the belief that there is no ortho dechlorination occurring in TCP. The ortho defluorination of TFP can be seen from the data presented in Figure 6. Under slower flow (1.0 mL/min > flow > 0.125 mL/min; Figure 6B−E), additional radicals are observed. For the data presented in Figure 6, species 2 can be simulated as a monofluorinated radical (a_o^F = 10.7 G) with two nonidentical protons (a_1^H = 1.99 G and a_2^H = 2.96 G), and species 3 can be simulated as an asymmetric radical (a proposed semiquinone) with two nonidentical protons (a_1^H = 1.86, a_2^H = 2.92) (Scheme 3, where R_a and R_b are ESR silent nuclei). Further investigation into the complete oxidation of TFP is required to fully understand the mechanism, although as a preliminary thought, it appears as though the radical−radical coupling reaction with TFP• involves the ether intermediate resulting from coupling at not only the para position but also the ortho position.

The ESR data requires additional discussion. Presented in Figure 4 are the experimental (4B) and simulated (4B′) spectra of TFP•. These IE-ESR data are extremely reproducible; IE-ESR data have no scan time-dependent features.[14] The simulation of these data fit very well with the only exception being the intensity of the outer ESR transitions (3460−3470 G and 3515−3525 G); the experimental intensity of the outer transitions is lower in amplitude than that of the simulated. The broadening of the higher field outer transitions (>3500 G) is a result of small hyperfine anisotropy commonly seen in ESR spectra with large hfcc, although the lower than expected intensity of the lowest and highest field lines (3460−3470 G and 3515−3525 G) remains unclear. Similar ESR observations have been seen by others for the fluoranil radical anion[26] and 9,10-perfluoroanthraquinone radical anion.[27]

In regard to the ESR simulation of the TCP•, the simulations did not require the use of both ^{35}Cl and ^{37}Cl isotopes. Reported simulations of TCP•[18] did use both isotopes, but this early publication did not have access to sophisticated computer methods. To further interpret the TCP• ESR data, the well-determined fluorine hfcc from TFP• (a_o^F = 13.5 G, a_p^F = 25.0 G)

were scaled using the gyromagnetic ratios to predict chlorine hfcc (a_o^{35Cl} = 1.4 G and a_p^{35Cl} = 2.6 G; a_o^{37Cl} = 1.2 G and a_p^{37Cl} = 2.2 G). These values, along with the *meta*-protons (a_m^{H} = 1.5 G) and natural isotopic abundance, were used to generate a predicted TCP• ESR spectrum. Two observations were made: (1) the predicted a_o^{Cl} and a_p^{Cl} from the scaled TFP• hfcc were larger than the observed, indicating that the spin density on the fluorine nuclei is slightly larger than that for the chlorine nuclei, and (2) an adequate simulation could be achieved using only the ^{35}Cl hfcc. When isotopic abundance of ^{35}Cl and ^{37}Cl was included in the simulation, the outermost lines were only slightly broadened. In our case, the low signal-to-noise in the high resolution ESR spectra (Figure 4A′,C′; Figure S1, Supporting Information) does not allow for clear observation of these outermost lines.

SUMMARY

We have detected the primary 2,4,6-trihalophenoxyl radical intermediates resulting from the 1-electron peroxidase oxidation of TCP, TFP, and DCFP. Since the observed IE-ESR spectra are isotropic, we conclude that the primary radicals are not associated with the reaction center and are free to react further in solution. The ESR data provide support for the hypothesis that the formation of DCQ involves a 1-electron peroxidase oxidation of the TCP, followed by radical coupling chemistry resulting in TCP^+, which is attacked by OH^- in solution to form DCQ and Cl^-. Secondary radicals observed under slower-flow IE-ESR experiments in both TCP (Figure 5) and TFP (Figure 6) are tentatively assigned as halogenated/dehalogenated 1,4-semiquinones; the mechanism of semiquinone formation will be presented in a subsequent paper.

ASSOCIATED CONTENT

Supporting Information. Details of the ESR simulation of TCP•/DCFP•; TFP• spectrum from dehaloperoxidase and myoglobin with kinetics. This material is available free of charge via the Internet at http://pubs.acs.org.

AUTHOR INFORMATION

Corresponding Author

*Tel: 309-457-2368. E-mail: besturgeon@monm.edu.

Funding Sources

This project was in part supported by a grant from the Research Corporation for Science Advancement: Cottrell College Science Award #7943 (B.E.S.) and U.S. Army Research Office grant #52278 (S.F.).

ACKNOWLEDGMENT

We wish to thank Garry R. Buettner and Brett A. Wagner of the University of Iowa ESR Facility and Ronald P. Mason and Jean Corbett of the National Institute of Environmental Sciences (NIEHS/NIH) for the use of ESR instrumentation and consultation. We wish to acknowledge Eric M. Todd of Monmouth College for review of the manuscript.

ABBREVIATIONS

TCP, 2,4,6-trichlorophenol; TCP•, 2,4,6-trichlorophenoxyl radical; TCP^+, 2,4,6-trichlorocyclohexadienone cation; TFP, 2,4,6-trifluorophenol; TFP•, 2,4,6-trifluorophenoxyl radical; DCFP, 2,6-dichloro-4-fluorophenol; DCFP•, 2,6-dichloro-4-fluorophenoxyl radical; XAOH, unspecified halophenol; XAO•, unspecified halophenoxyl radical ; XAO^+, unspecified halocyclohexadienone cation; DCQ, 2,6-dichloro-1,4-benzoquinone; HRP, horseradish peroxidase; RS, enzyme resting state; HRP_i, immobilized HRP; hfcc, hyperfine coupling constants; IE-ESR, immobilized enzyme ESR

REFERENCES

(1) Hammel, K. E., and Tardone, P. J. (1988) The oxidative 4-dechlorination of polychlorinated phenols is catalyzed by extracellular fungal lignin peroxidases. *Biochemistry 27*, 6563–6568.

(2) Wiese, F. W., Chang, H. C., Lloyd, R. V., Freeman, J. P., and Samokyszyn, V. M. (1998) Peroxidase-catalyzed oxidation of 2,4,6-trichlorophenol. *Arch. Environ. Contam. Toxicol. 34*, 217–222.

(3) Ferrari, R. P., Laurenti, E., and Trotta, F. (1999) Oxidative 4-dechlorination of 2,4,6-trichlorophenol catalyzed by horseradish peroxidase. *J. Biol. Inorg. Chem. 4*, 232–237.

(4) Osborne, R. L., Raner, G. M., Hager, L. P., and Dawson, J. H. (2006) C. fumago chloroperoxidase is also a dehaloperoxidase: oxidative dehalogenation of halophenols. *J. Am. Chem. Soc. 128*, 1036–1037.

(5) Osborne, R. L., Coggins, M. K., Terner, J., and Dawson, J. H. (2007) Caldariomyces fumago chloroperoxidase catalyzes the oxidative dehalogenation of chlorophenols by a mechanism involving two one-electron steps. *J. Am. Chem. Soc. 129*, 14838–14839.

(6) Chen, Y. P., Woodin, S. A., Lincoln, D. E., and Lovell, C. R. (1996) An unusual dehalogenating peroxidase from the marine terebellid polychaete *Amphitrite ornata*. *J. Biol. Chem. 271*, 4609–4612.

(7) Osborne, R. L., Coggins, M. K., Walla, M., and Dawson, J. H. (2007) Horse heart myoglobin catalyzes the H2O2-dependent oxidative dehalogenation of chlorophenols to DNA-binding radicals and quinones. *Biochemistry 46*, 9823–9829.

(8) Dunford, H. B. (1999) *Heme Peroxidases*, Wiley-VCH, New York.

(9) Feducia, J., Dumarieh, R., Gilvey, L. B., Smirnova, T., Franzen, S., and Ghiladi, R. A. (2009) Characterization of dehaloperoxidase compound ES and its reactivity with trihalophenols. *Biochemistry 48*, 995–1005.

(10) Roman, R., and Dunford, H. B. (1972) pH Dependence of the oxidation of iodide by compound I of horseradish peroxidase. *Biochemistry 11*, 2076–2082.

(11) Roman, R., and Dunford, H. B. (1973) Studies on horseradish peroxidase. XII. A kinetic study of the oxidation of sulfite and nitrite by compounds I and II. *Can. J. Chem. 51*, 588–596.

(12) Belyea, J., Gilvey, L. B., Davis, M. F., Godek, M., Sit, T. L., Lommel, S. A., and Franzen, S. (2005) Enzyme function of the globin dehaloperoxidase from *Amphitrite ornata* is activated by substrate binding. *Biochemistry 44*, 15637–15644.

(13) Harris, D. C. (2006) *Quantitative Chemical Analysis*, 7th ed., W. H. Freeman and Company, New York.

(14) Sturgeon, B. E., Chen, Y. R., and Mason, R. P. (2003) Immobilized enzyme electron spin resonance: a method for detecting enzymatically generated transient radicals. *Anal. Chem. 75*, 5006–5011.

(15) Duling, D. R. (1994) Simulation of multiple isotropic spin-trap EPR spectra. *J. Magn. Reson. 104*, 105–110.

(16) Chen, Y. R., Deterding, L. J., Sturgeon, B. E., Tomer, K. B., and Mason, R. P. (2002) Protein oxidation of cytochrome c by reactive halogen species enhances its peroxidase activity. *J. Biol. Chem. 277*, 29781–29791.

(17) Sturgeon, B. E., Glover, R. E., Chen, Y. R., Burka, L. T., and Mason, R. P. (2001) Tyrosine iminoxyl radical formation from tyrosyl radical/nitric oxide and nitrosotyrosine. *J. Biol. Chem. 276*, 45516–45521.

(18) Graf, F., Loth, K., and Guenthard, H. H. (1977) Chlorine hyperfine splittings and spin density distributions of phenoxy radicals. An ESR and quantum chemical study. *Helv. Chim. Acta 60*, 710–721.

(19) Sealy, R. C., Harman, L., West, P. R., and Mason, R. P. (1985) The electron-spin resonance-spectrum of the tyrosyl radical. *J. Am. Chem. Soc. 107*, 3401–3406.

(20) Mottley, C., and Mason, R. P. (2001) Sulfur-centered radical formation from the antioxidant dihydrolipoic acid. *J. Biol. Chem. 276*, 42677–42683.

(21) Jacob, J. S., Cistola, D. P., Hsu, F. F., Muzaffar, S., Mueller, D. M., Hazen, S. L., and Heinecke, J. W. (1996) Human phagocytes employ the myeloperoxidase-hydrogen peroxide system to synthesize dityrosine, trityrosine, pulcherosine, and isodityrosine by a tyrosyl radical-dependent pathway. *J. Biol. Chem. 271*, 19950–19956.

(22) Bors, W., and Buettner, G. R. (1997) The vitamin C radical and its reactions, in *Vitamin C in Health and Disease* (Packer, L., and Fuchs, J., Eds.) pp 75−94, Marcel Dekker, Inc., New York.

(23) Song, Y., Buettner, G. R., Parkin, S., Wagner, B. A., Robertson, L. W., and Lehmler, H. J. (2008) Chlorination increases the persistence of semiquinone free radicals derived from polychlorinated biphenyl hydroquinones and quinones. *J. Org. Chem. 73*, 8296–8304.

(24) Song, Y., Wagner, B. A., Lehmler, H. J., and Buettner, G. R. (2008) Semiquinone radicals from oxygenated polychlorinated biphenyls: electron paramagnetic resonance studies. *Chem. Res. Toxicol. 21*, 1359–1367.

(25) Wong, S. K., Sytnyk, W., and Wan, J. K. S. (1972) Electron spin resonance study of the self-disproportionation of some semiquinone radicals in solution. *Can. J. Chem. 50*, 3052–3057.

(26) Lubitz, W., Dinse, K. P., Moebius, K., and Biehl, R. (1975) Fluorine and proton ENDOR of aromatic radicals in solution. *Chem. Phys. 8*, 371–383.

(27) Rakitin, A. R., Yff, D., and Trapp, C. (2003) Fluorine hyperfine splittings in the electron spin resonance (ESR) spectra of aromatic radicals. An experimental and theoretical investigation. *J. Phys. Chem. A 107*, 6281–6292.